Composite Structures 131 (2015) 810–820

Contents lists available at ScienceDirect

Composite Structures

journal homepage: www.elsevier.com/locate/compstruct

Closed-form solutions for nonlinear bending and free vibration of functionally graded microplates based on the modified couple stress theory

Jia Lou, Liwen He *

Piezoelectric Device Laboratory, Department of Mechanics and Engineering Science, Ningbo University, Ningbo, Zhejiang 315211, China
Changchun Institute of Optics, Fine Mechanics and Physics, Chinese Academy of Sciences, Changchun 130033, China

ARTICLE INFO

Article history:
Available online 20 June 2015

Keywords:
Functionally graded microplate
Modified couple stress theory
Physical neutral surface
Galerkin method
Nonlinear bending
Nonlinear vibration

ABSTRACT

In this paper, the nonlinear bending and free vibration responses of a simply supported functionally graded (FG) microplate lying on an elastic foundation are studied within the framework of the modified couple stress theory and the Kirchhoff/Mindlin plate theory together with the von Karman's geometric nonlinearity. The equations of motion and boundary conditions for the FG microplate are derived from the Hamilton's principle. Due to introducing the physical neutral surface, there is no stretching-bending coupling in the constitutive equations, and the equations of motion become simpler. By using the Galerkin method, the equations of motion are reduced to nonlinear algebraic equations and ordinary differential equations (ODEs) for the bending and vibration problems respectively. By solving the algebraic equations, closed-form solutions for the nonlinear bending deflection of the microplate are derived. Closed-form solutions for the nonlinear vibration frequency are also obtained by applying He's variational method to the ODEs. Based on the obtained closed-form solutions, numerical examples are further presented to investigate the effects of the material length scale parameter to thickness ratio, the length to thickness ratio, the power law index and the elastic foundation on the nonlinear bending and free vibration responses of the microplate.

1. Introduction

Functionally graded materials (FGMs), as a new class of composites with physical properties varying smoothly and continuously from one surface to another, have drawn extensive attention owing to their excellent performances such as thermal protection from ablation and elimination of stress concentration [1,2]. Recently, FGMs have been spread in micro- and nano-electro-mechanical systems (MEMS/NEMS) and atomic force microscopes (AFMs) to achieve high sensitivity and desired performances [3]. In these applications, functionally graded (FG) microbeams and microplates are widely used as fundamental structural elements. It is experimentally observed that these microstructures exhibit size-dependent mechanical behavior, which is usually called “size effects”. It is therefore of prime importance to take the size effects into consideration in the analyses of the mechanical behavior of FG microstructures. However, classical continuum theories cannot account for the size effects due to the lack of an intrinsic material length scale parameter. Therefore, it is necessary to adopt size-dependent continuum theories, such as the nonlocal elasticity theory [4], the strain gradient theory [5,6], the classical couple stress theory [7–9] and its modified version [10], to investigate the mechanical responses of microstructures.

Among all these size-dependent continuum theories, the modified couple stress theory (MCST) proposed by Yang et al. [10] has the advantage of involving only one material length scale parameter. Based on the MCST, several non-classical beam and plate models have been developed to capture the size effects in microstructures. For example, Park and Gao [11] developed a Euler–Bernoulli beam model for the bending analysis of nanobeams. Kong et al. [12] and Kahrobaiyan et al. [13] employed the same model to study the vibration behavior of microbeams. Ma et al. [14] developed a Timoshenko beam model to incorporate the effect of transverse shear deformation. This model was also adopted for the buckling analysis of microtubules [15] and the vibration analysis of nanotubes [16]. Ma et al. [17] further developed a size-dependent non-classical Reddy–Levinson beam model and studied the static bending and free vibration problems of microbeams. Besides these non-classical beam models, various

* Corresponding author.
E-mail addresses: jiajia_smile@163.com (J. Lou), physi_mechanism@163.com (L. He).

http://dx.doi.org/10.1016/j.compstruct.2015.06.031
0263-8223/

size-dependent plate models based on the MCST have also been developed. Tsiatas [18] first developed a Kirchhoff plate model for the static bending analysis of microplates. This model was then used for the free vibration analysis of microplates [19,20]. Ke et al. [21] developed a Mindlin microplate model based on the MCST and studied the free vibration behavior of microplates. To ensure that the transverse shear stresses on the top and bottom surfaces of microplates vanish and thus improve the calculation accuracy, a higher order size-dependent model based on Reddy's third order shear deformation theory was developed by Thai and Kim [22] for the bending and free vibration analyses of FG microplates. Furthermore, Kim and Reddy [23] developed a general third-order plate model by relaxing the hypothesis of inextensiblity transverse normals and presented analytical solutions for bending, buckling and vibration problems.

The above studies indicate that although significant progress has been made on investigating the size-dependent behavior of microstructures by using the MCST and various beam and plate theories, they are all limited to linear analyses. In fact, in many cases large deformation and rotation take place within microstructures, where the geometric nonlinearity should be taken into account. Motivated by these nonlinear problems, many works have been devoted to exploring the nonlinear mechanical behavior of microstructures. Xia et al. [24] developed a nonlinear non-classical Euler–Bernoulli beam model and studied the static bending, postbuckling and free vibration behavior of simply supported mircobeams. This model was also employed by Simsek [25] to study the nonlinear bending and vibration behavior of microbeams lying on an elastic foundation. Asghari et al. [26] proposed a nonlinear size-dependent Timoshenko beam model and studied the nonlinear bending and free vibration behavior of simply supported microbeams. In addition to these studies, the nonlinear mechanical behavior of microplates has also been studied by some researchers. Reddy and Berry [27] developed Kirchhoff and Mindlin plate theories for the nonlinear axisymmetric bending problem of circular FG microplates. Based on the Kirchhoff plate theory (KPT), Wang et al. [28] studied the nonlinear axisymmetric free vibration response of a circular microplate by using Kantorvich and shooting methods. Ke et al. [3,29] used the Mindlin plate theory (MPT) to investigate the axisymmetric postbuckling and nonlinear free vibration problems of annular FG microplates. The postbuckling path and nonlinear frequencies were obtained with the help of the differential quadrature method in their work. Ansari et al. [30] also used the MPT and the generalized differential quadrature method to explore the nonlinear vibration behavior of rectangular FG microplates. Furthermore, Reddy and Kim [31] developed a nonlinear third-order plate theory that accounts for the size effects and the material gradation through the thickness of a FG microplate. However, no analytical solutions for the nonlinear mechanical responses of microplates have been presented in these studies. Recently, Thai and Choi [32] presented an approximate analytical solution for the nonlinear bending deflection of an isotropic Kirchhoff microplate under transverse loads.

The above review indicates that the nonlinear mechanical behavior of FG microplates is not fully explored and needs further research. To the best of the authors' knowledge, simple closed-form solutions for the nonlinear bending and free vibration problems of FG microplates accounting for the couple stress effect have not been reported yet. The present work attempts to obtain simple closed-form solutions for the nonlinear bending deflection and vibration frequency of a simply supported rectangular FG microplate lying on an elastic foundation. Firstly, the governing equations for the FG microplate are derived from the Hamilton's principle based on the MCST, the Kirchhoff/Mindlin plate theory, and the von Karman's geometric nonlinearity. And then, the equations of motion are reduced to nonlinear algebraic equations and ordinary differential equations for the bending and free vibration problems respectively by using the Galerkin method. Afterwards, by solving the algebraic equations, analytical solutions for the nonlinear bending deflection are obtained, and analytical formulas for the nonlinear vibration frequency are also derived by applying He's variational method to the ordinary differential equations. In addition, the obtained solutions are validated by comparing with published results. Finally, numerical studies are performed to investigate the effects of the material length scale parameter to thickness ratio, the length to thickness ratio, the power law index and the elastic foundation on the nonlinear bending and free vibration responses of the microplate in detail.

2. Formulation

As shown in Fig. 1, a rectangular FG microplate with length a, width b, and thickness h is considered. The microplate is lying on an elastic foundation with transverse stiffness coefficient K_L, shear stiffness coefficient K_P, and nonlinear stiffness coefficient K_{NL} respectively. All the four edges of the microplate are simply supported. The material properties of the microplate such as Young's modulus E and mass density ρ are assumed to vary continuously through the thickness by a power law as:

$$E(z) = E_2 + (E_1 - E_2)\left(\frac{1}{2} + \frac{z}{h}\right)^p, \quad \rho(z) = \rho_2 + (\rho_1 - \rho_2)\left(\frac{1}{2} + \frac{z}{h}\right)^p, \tag{1}$$

where the subscripts 1 and 2 represent the two materials used, and p is the power law index indicating the volume fractions of the component materials, while Poisson's ratio ν is assumed to be constant in this paper.

Introducing the physical neutral surface at $z = z_0$ as shown in Fig. 1, the displacement fields for the FG microplate based on the KPT and the MPT are expressed by Eqs. (2) and (3), respectively.

$$u_1 = u - (z - z_0)\frac{\partial w}{\partial x}, \quad u_2 = v - (z - z_0)\frac{\partial w}{\partial y}, \quad u_3 = w, \tag{2}$$

$$u_1 = u + (z - z_0)\varphi_x, \quad u_2 = v + (z - z_0)\varphi_y, \quad u_3 = w, \tag{3}$$

where (u, v, w) are the displacements on the physical neutral surface, (u_1, u_2, u_3) are the displacements at any point in the microplate, (φ_x, φ_y) are the rotations of the normal about y and x axes, respectively, and z_0 is defined as

$$z_0 = \frac{\int_{-h/2}^{h/2} E(z) z \mathrm{d}z}{\int_{-h/2}^{h/2} E(z) \mathrm{d}z}. \tag{4}$$

Eq. (4) indicates that the position of the physical neutral surface varies with the material distribution through the thickness. For a

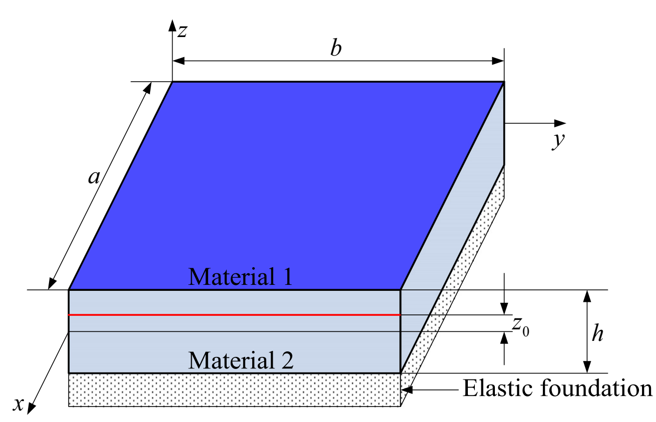

Fig. 1. A FG microplate lying on an elastic foundation.

homogenous plate or symmetrical laminated plate, the physical neutral surface coincides with the geometrical neutral surface, but for a FG plate with asymmetric material distribution, the physical neutral surface no longer coincides with the geometrical neutral surface [33].

Based on the assumed displacements in Eqs. (2) and (3), the motion equations in terms of displacements as well as the boundary conditions can be derived by using the Hamilton's principle. The detailed derivation process can refer to Thai and Choi's work [32]. The equations of motion and simply supported boundary conditions for FG microplates without body forces, body couples, and tangential tractions on the top and bottom surfaces are given below. In the rest of this paper, the FG microplate analyzed by using the KPT is termed as the Kirchhoff microplate, and the FG microplate analyzed by using the MPT is called the Mindlin microplate.

2.1. Governing equations for the Kirchhoff microplate

The equations of motion for the Kirchhoff microplate are written as:

$$A\left(\frac{\partial^2 u}{\partial x^2}+\frac{1-\nu}{2}\frac{\partial^2 u}{\partial y^2}+\frac{1+\nu}{2}\frac{\partial^2 v}{\partial x\partial y}\right)+\frac{A_n}{4}\nabla^2\left(\frac{\partial^2 v}{\partial x\partial y}-\frac{\partial^2 u}{\partial y^2}\right)+A\left[\frac{\partial w}{\partial x}\frac{\partial^2 w}{\partial x^2}+\nu\frac{\partial w}{\partial y}\frac{\partial^2 w}{\partial x\partial y}+\frac{1-\nu}{2}\left(\frac{\partial w}{\partial y}\frac{\partial^2 w}{\partial x\partial y}+\frac{\partial w}{\partial x}\frac{\partial^2 w}{\partial y^2}\right)\right]=I_0\ddot{u}-I_1\frac{\partial \ddot{w}}{\partial x},\tag{5a}$$

$$A\left(\frac{\partial^2 v}{\partial y^2}+\frac{1-\nu}{2}\frac{\partial^2 v}{\partial x^2}+\frac{1+\nu}{2}\frac{\partial^2 u}{\partial x\partial y}\right)+\frac{A_n}{4}\nabla^2\left(\frac{\partial^2 u}{\partial x\partial y}-\frac{\partial^2 v}{\partial x^2}\right)+A\left[\frac{\partial w}{\partial y}\frac{\partial^2 w}{\partial y^2}+\nu\frac{\partial w}{\partial x}\frac{\partial^2 w}{\partial x\partial y}+\frac{1-\nu}{2}\left(\frac{\partial w}{\partial x}\frac{\partial^2 w}{\partial x\partial y}+\frac{\partial w}{\partial y}\frac{\partial^2 w}{\partial x^2}\right)\right]=I_0\ddot{v}-I_1\frac{\partial \ddot{w}}{\partial y},\tag{5b}$$

$$-(D+A_n)\nabla^4 w+N-K_L w+K_p\nabla^2 w-K_{NL}w^3+q=I_0\ddot{w}+I_1\left(\frac{\partial \ddot{u}}{\partial x}+\frac{\partial \ddot{v}}{\partial y}\right)-I_2\nabla^2\ddot{w},\tag{5c}$$

where (A, D) are the classical stretching and bending stiffness coefficients, A_n is an additional stiffness which is contributed by the couple stress effect and has the same dimension with the classical bending stiffness, (I_0, I_1, I_2) are the mass inertias, q is the transverse load, the dot-superscript indicates differentiation with respect to the time variable t, and

$$(A,D)=\int_{-h/2}^{h/2}\frac{E(z)}{1-\nu^2}\left(1,(z-z_0)^2\right)dz,\ A_n=l^2\frac{1-\nu}{2}A,\tag{6}$$

$$(I_0,I_1,I_2)=\int_{-h/2}^{h/2}\rho(z)\left(1,z-z_0,(z-z_0)^2\right)dz,\tag{7}$$

$$N=\frac{\partial}{\partial x}\left(N_x\frac{\partial w}{\partial x}+N_{xy}\frac{\partial w}{\partial y}\right)+\frac{\partial}{\partial y}\left(N_{xy}\frac{\partial w}{\partial x}+N_y\frac{\partial w}{\partial y}\right),\tag{8}$$

$$\begin{Bmatrix}N_x\\N_y\\N_{xy}\end{Bmatrix}=A\begin{bmatrix}1&\nu&0\\\nu&1&0\\0&0&(1-\nu)/2\end{bmatrix}\begin{Bmatrix}\frac{\partial u}{\partial x}+\frac{1}{2}\left(\frac{\partial w}{\partial x}\right)^2\\\frac{\partial v}{\partial y}+\frac{1}{2}\left(\frac{\partial w}{\partial y}\right)^2\\\frac{\partial u}{\partial y}+\frac{\partial v}{\partial x}+\frac{\partial w}{\partial x}\frac{\partial w}{\partial y}\end{Bmatrix},\tag{9}$$

in which l is the material length scale parameter which is regarded as a material property measuring the couple stress effect. It should be noted that by introducing the physical neutral surface, the classical stretching-bending coupling stiffness defined as $B=\int_{-h/2}^{h/2}E(z)(z-z_0)/(1-\nu^2)dz$ vanishes. In the present work, the first-order mass moment I_1 is neglected for its contribution is relatively small, and the in-plane inertial forces are also neglected [34,35].

It is assumed that each one of the four edges is immovable in its normal direction, but freely movable in its tangential direction. Thus the simply supported boundary conditions of the Kirchhoff microplate can be written as:

$$x=0,\ a:\ u=\frac{\partial v}{\partial x}=w=\frac{\partial^2 w}{\partial x^2}=0;\ \ y=0,\ b:\ v=\frac{\partial u}{\partial y}=w=\frac{\partial^2 w}{\partial y^2}=0.\tag{10}$$

The displacements (u, v, w) are assumed to take the following forms [36]:

$$\begin{aligned}u(x,y,t)&=\frac{1}{16}\alpha W_{mn}^2(t)\sin(2\alpha x)\left[\cos(2\beta y)-1+\nu\beta^2/\alpha^2\right],\\v(x,y,t)&=\frac{1}{16}\beta W_{mn}^2(t)\left[\cos(2\alpha x)-1+\nu\alpha^2/\beta^2\right]\sin(2\beta y),\\w(x,y,t)&=W_{mn}(t)\sin(\alpha x)\sin(\beta y).\end{aligned}\tag{11}$$

Clearly, this choice of displacements satisfies the simply supported boundary conditions of the Kirchhoff microplate, and the expressions of (u, v, w) also satisfy Eqs. (5a) and (5b) automatically. In order to find the solution of the partial differential Eqs. (5), the Galerkin method is utilized to reduce Eq. (5c). By substituting the expressions of (u, v, w) in Eq. (11) into Eq. (5c), the residue Λ is obtained as:

$$\Lambda=\left\{-\left\{\frac{A}{16}\left[4\nu\alpha^2\beta^2+2(\alpha^4+\beta^4)+2(\nu^2-1)(\alpha^4\cos 2\beta y+\beta^4\cos 2\alpha x)\right]+\frac{9}{16}K_{NL}\right\}W_{mn}^3-\left[(D+A_n)(\alpha^2+\beta^2)^2+K_L+K_P(\alpha^2+\beta^2)\right]W_{mn}-\left[I_0+I_2(\alpha^2+\beta^2)\right]\ddot{W}_{mn}\right\}\sin(\alpha x)\sin(\beta y)+q.\tag{12}$$

The transverse load q can be expanded into the following double Fourier sine series:

$$q(x,y)=\sum_{m=1}^{\infty}\sum_{n=1}^{\infty}Q_{mn}\sin(\alpha x)\sin(\beta y),\tag{13}$$

where $\alpha=m\pi/a,\ \beta=n\pi/b$, and

$$Q_{mn}=\frac{4}{ab}\int_0^a\int_0^b q(x,y)\sin(\alpha x)\sin(\beta y)dy\,dx.\tag{14}$$

For a sinusoidal load of intensity q_0, the coefficient $Q_{11}=q_0$, and all other coefficients $Q_{mn}(m\neq 1$ or $n\neq 1)$ equal to zero.

Substituting Eq. (13) into Eq. (12) and setting the integral $\int_0^a\int_0^b\Lambda\sin(\alpha x)\sin(\beta y)dydx$ to zero, the following equation is obtained:

$$\left\{\frac{A}{16}\left[4\nu\alpha^2\beta^2+(3-\nu^2)(\alpha^4+\beta^4)\right]+\frac{9}{16}K_{NL}\right\}W_{mn}^3+\left[(D+A_n)(\alpha^2+\beta^2)^2+K_L+K_P(\alpha^2+\beta^2)\right]W_{mn}+\left[I_0+I_2(\alpha^2+\beta^2)\right]\ddot{W}_{mn}=Q_{mn}.\tag{15}$$

This equation will be used in Section 2.3 to derive analytical solutions for the nonlinear bending deflection and vibration frequency of the Kirchhoff microplate.

2.2. Governing equations for the Mindlin microplate

The equations of motion for the Mindlin microplate are expressed as follows:

$$A\left(\frac{\partial^2 u}{\partial x^2}+\frac{1-v}{2}\frac{\partial^2 u}{\partial y^2}+\frac{1+v}{2}\frac{\partial^2 v}{\partial x\partial y}\right)+\frac{A_n}{4}\nabla^2\left(\frac{\partial^2 v}{\partial x\partial y}-\frac{\partial^2 u}{\partial y^2}\right)+A\left[\frac{\partial w}{\partial x}\frac{\partial^2 w}{\partial x^2}+v\frac{\partial w}{\partial y}\frac{\partial^2 w}{\partial x\partial y}+\frac{1-v}{2}\left(\frac{\partial w}{\partial y}\frac{\partial^2 w}{\partial x\partial y}+\frac{\partial w}{\partial x}\frac{\partial^2 w}{\partial y^2}\right)\right]=I_0\ddot{u}+I_1\ddot{\varphi}_x, \tag{16a}$$

$$A\left(\frac{\partial^2 v}{\partial y^2}+\frac{1-v}{2}\frac{\partial^2 v}{\partial x^2}+\frac{1+v}{2}\frac{\partial^2 u}{\partial x\partial y}\right)+\frac{A_n}{4}\nabla^2\left(\frac{\partial^2 u}{\partial x\partial y}-\frac{\partial^2 v}{\partial x^2}\right)+A\left[\frac{\partial w}{\partial y}\frac{\partial^2 w}{\partial y^2}+v\frac{\partial w}{\partial x}\frac{\partial^2 w}{\partial x\partial y}+\frac{1-v}{2}\left(\frac{\partial w}{\partial x}\frac{\partial^2 w}{\partial x\partial y}+\frac{\partial w}{\partial y}\frac{\partial^2 w}{\partial x^2}\right)\right]=I_0\ddot{v}+I_1\ddot{\varphi}_y, \tag{16b}$$

$$A_{44}\left(\frac{\partial\varphi_x}{\partial x}+\frac{\partial\varphi_y}{\partial y}+\nabla^2 w\right)-\frac{A_n}{4}\nabla^4 w+\frac{A_n}{4}\nabla^2\left(\frac{\partial\varphi_x}{\partial x}+\frac{\partial\varphi_y}{\partial y}\right)+N-K_L w+K_p\nabla^2 w-K_{NL}w^3+q=I_0\ddot{w}, \tag{16c}$$

$$D\left(\frac{\partial^2\varphi_x}{\partial x^2}+\frac{1-v}{2}\frac{\partial^2\varphi_x}{\partial y^2}+\frac{1+v}{2}\frac{\partial^2\varphi_y}{\partial x\partial y}\right)-A_{44}\left(\varphi_x+\frac{\partial w}{\partial x}\right)-\frac{A_n}{4}\nabla^2\frac{\partial w}{\partial x}+\frac{A_n}{4}\left(\frac{\partial^2\varphi_x}{\partial x^2}+4\frac{\partial^2\varphi_x}{\partial y^2}-3\frac{\partial^2\varphi_y}{\partial x\partial y}\right)+\frac{D_n}{4}\nabla^2\left(\frac{\partial^2\varphi_y}{\partial x\partial y}-\frac{\partial^2\varphi_x}{\partial y^2}\right)=I_1\ddot{u}+I_2\ddot{\varphi}_x, \tag{16d}$$

$$D\left(\frac{\partial^2\varphi_y}{\partial y^2}+\frac{1-v}{2}\frac{\partial^2\varphi_y}{\partial x^2}+\frac{1+v}{2}\frac{\partial^2\varphi_x}{\partial x\partial y}\right)-A_{44}\left(\varphi_y+\frac{\partial w}{\partial y}\right)-\frac{A_n}{4}\nabla^2\frac{\partial w}{\partial y}+\frac{A_n}{4}\left(\frac{\partial^2\varphi_y}{\partial y^2}+4\frac{\partial^2\varphi_y}{\partial x^2}-3\frac{\partial^2\varphi_x}{\partial x\partial y}\right)+\frac{D_n}{4}\nabla^2\left(\frac{\partial^2\varphi_x}{\partial x\partial y}-\frac{\partial^2\varphi_y}{\partial x^2}\right)=I_1\ddot{v}+I_2\ddot{\varphi}_y, \tag{16e}$$

where A_{44} is the shear stiffness of the Mindlin microplate defined as$A_{44}=k_sA(1-v)/2$, in which k_s is the shear correction factor whose value is chosen to be 5/6, and D_n, which is defined as $D_n=l^2(1-v)D/2$, is a higher-order stiffness contributed by the couple stress effect.

Similarly, the simply supported boundary conditions of the Mindlin microplate can be written as:

$$x=0,\ a:\ u=\frac{\partial v}{\partial x}=w=\varphi_y=\frac{\partial\varphi_x}{\partial x}=0;\qquad y=0,\ b:\ v=\frac{\partial u}{\partial y}=w=\varphi_x=\frac{\partial\varphi_y}{\partial y}=0. \tag{17}$$

The generalized displacements $\left(u,v,w,\varphi_x,\varphi_y\right)$ are assumed as [36]:

$$\begin{aligned}
u(x,y,t)&=\frac{1}{16}\alpha W_{mn}^2(t)\sin(2\alpha x)\left[\cos(2\beta y)-1+v\beta^2/\alpha^2\right],\\
v(x,y,t)&=\frac{1}{16}\beta W_{mn}^2(t)\left[\cos(2\alpha x)-1+v\alpha^2/\beta^2\right]\sin(2\beta y),\\
w(x,y,t)&=W_{mn}(t)\sin(\alpha x)\sin(\beta y),\\
\varphi_x(x,y,t)&=\psi_{xmn}(t)\cos(\alpha x)\sin(\beta y),\\
\varphi_y(x,y,t)&=\psi_{ymn}(t)\sin(\alpha x)\cos(\beta y).
\end{aligned} \tag{18}$$

Evidently, this choice of generalized displacements satisfies the simply supported boundary conditions of the Mindlin microplate, and the expressions of (u,v,w) also satisfy Eqs. (16a) and (16b) automatically. Differentiating Eqs. (16d) and (16e) with respect to x and y respectively and adding up the two obtained equations, the following equation is obtained:

$$\left(D+\frac{A_n}{4}\right)\nabla^2\phi-\frac{A_n}{4}\nabla^4 w-A_{44}\left(\phi+\nabla^2 w\right)=I_2\ddot{\phi}, \tag{19}$$

where

$$\phi=\frac{\partial\varphi_x}{\partial x}+\frac{\partial\varphi_y}{\partial y}=\Phi_{mn}(t)\sin(\alpha x)\sin(\beta y) \tag{20}$$

in which $\Phi_{mn}=-(\alpha\psi_{xmn}+\beta\psi_{ymn})$.

Adding Eq. (19) to Eq. (16c) yields:

$$\left(D+\frac{A_n}{2}\right)\nabla^2\phi-\frac{A_n}{2}\nabla^4 w+N-K_L w+K_p\nabla^2 w-K_{NL}w^3+q=I_0\ddot{w}+I_2\ddot{\phi}. \tag{21}$$

Performing the following variable transformations:

$$\Phi_{mn}(t)=\left(\alpha^2+\beta^2\right)W_{1mn}(t),\quad W_{mn}(t)=W_{1mn}(t)+W_{2mn}(t), \tag{22}$$

substituting Eqs. (13), (18), (20) and (22) into Eqs. (21) and (16c), and using the Galerkin approach, the following two equations are obtained:

$$k_{11}W_{1mn}+k_{12}W_{2mn}+k_{13}(W_{1mn}+W_{2mn})^3-Q_{mn}+m_{11}\ddot{W}_{1mn}+m_{12}\ddot{W}_{2mn}=0, \tag{23a}$$

$$k_{12}W_{1mn}+k_{22}W_{2mn}+k_{13}(W_{1mn}+W_{2mn})^3-Q_{mn}+m_{12}\ddot{W}_{1mn}+m_{22}\ddot{W}_{2mn}=0 \tag{23b}$$

in which

$$\begin{aligned}
k_{11}&=(D+A_n)\left(\alpha^2+\beta^2\right)^2+K_L+K_p\left(\alpha^2+\beta^2\right),\\
k_{12}&=\frac{A_n}{2}\left(\alpha^2+\beta^2\right)^2+K_L+K_p\left(\alpha^2+\beta^2\right),\\
k_{13}&=\frac{A}{16}\left[4v\alpha^2\beta^2+\left(3-v^2\right)\left(\alpha^4+\beta^4\right)\right]+\frac{9}{16}K_{NL},\\
k_{22}&=\frac{A_n}{4}\left(\alpha^2+\beta^2\right)^2+A_{44}\left(\alpha^2+\beta^2\right)+K_L+K_p\left(\alpha^2+\beta^2\right),\\
m_{11}&=I_0+I_2\left(\alpha^2+\beta^2\right),\ m_{12}=I_0,\ m_{22}=I_0.
\end{aligned} \tag{24}$$

Eqs. (23) will be used in Section 2.4 to derive analytical formulas for the nonlinear bending deflection and vibration frequency of the Mindlin microplate.

It should be noted that the equations of motion for the Kirchhoff/Mindlin microplate derived in the present paper are slightly different from those derived by Thai and Choi [32]. The differences are due to the fact that in the present paper the effect of the elastic foundation is taken into account and the in-plane generalized displacements u and v are defined on the physical neutral surface instead of the geometrical neutral surface. Therefore, there is no stretching-bending coupling in the constitutive equations, and the equations of motion take similar forms with those of a homogeneous isotropic microplate.

2.3. Analytical solutions for the deflection and frequency of the Kirchhoff microplate

The nonlinear bending and vibration responses of a simply supported FG microplate are studied based on the KPT in this subsection. For the static bending problem, the displacements are independence of time, thus the inertial item in Eq. (15) vanishes. Only the case of a sinusoidal load of intensity q_0 acting on the FG microplate is considered here. According to Eq. (15), the nonlinear deflection of the Kirchhoff microplate W_{KNL} can be obtained by solving the following algebraic equation:

$$\left\{\frac{A}{16}\left[4\nu\alpha^2\beta^2+(3-\nu^2)(\alpha^4+\beta^4)\right]+\frac{9}{16}K_{NL}\right\}W_{KNL}^3 + \left[(D+A_n)(\alpha^2+\beta^2)^2+K_L+K_P(\alpha^2+\beta^2)\right]W_{KNL}=q_0. \quad (25)$$

Eq. (25) gives two complex conjugate roots and a real root, and only the real root represents the bending deflection of the Kirchhoff microplate. Therefore the bending deflection of the microplate can be obtained as:

$$W_{KNL}=-a_1\left(\frac{27}{2}\bar{q}_0+\frac{3}{2}\sqrt{12a_1^3+81\bar{q}_0^2}\right)^{-1/3} + \left(\frac{1}{2}\bar{q}_0+\frac{1}{18}\sqrt{12a_1^3+81\bar{q}_0^2}\right)^{1/3}, \quad (26)$$

where

$$a_1=\frac{(D+A_n)(\alpha^2+\beta^2)^2+K_L+K_P(\alpha^2+\beta^2)}{\frac{A}{16}\left[4\nu\alpha^2\beta^2+(3-\nu^2)(\alpha^4+\beta^4)\right]+\frac{9}{16}K_{NL}},\quad \bar{q}_0=\frac{q_0}{\frac{A}{16}\left[4\nu\alpha^2\beta^2+(3-\nu^2)(\alpha^4+\beta^4)\right]+\frac{9}{16}K_{NL}}. \quad (27)$$

The linear deflection of the Kirchhoff microplate can be easily derived from Eq. (25) as:

$$W_{KL}=\frac{q_0}{(D+A_n)(\alpha^2+\beta^2)^2+K_L+K_P(\alpha^2+\beta^2)}. \quad (28)$$

It should be noted that the first term on the left-hand side of Eq. (25), which is contributed from the von Karman's geometric nonlinearity and the nonlinear stiffness of the elastic foundation, is proportional to the third power of W_{KNL}. Consequently, the nonlinear stiffness (defined as q_0/W_{KNL}) of the FG microplate, in contrast to the constant linear stiffness (defined as q_0/W_{KL}), increases with the increase of the deflection. This is the so called "intrinsic stiffening effect".

For the free vibration problem, Eq. (15) is written as:

$$\ddot{W}(t)+(D_1+D_2+D_3)W(t)+(D_4+D_5)W^3(t)=0 \quad (29)$$

in which the coefficients are defined as:

$$D_1=\frac{(D+A_n)(\alpha^2+\beta^2)^2}{I_0+I_2(\alpha^2+\beta^2)},\quad D_2=\frac{K_L}{I_0+I_2(\alpha^2+\beta^2)},$$
$$D_3=\frac{K_P(\alpha^2+\beta^2)}{I_0+I_2(\alpha^2+\beta^2)},\quad D_4=\frac{(A/16)\left[4\nu\alpha^2\beta^2+(3-\nu^2)(\alpha^4+\beta^4)\right]}{I_0+I_2(\alpha^2+\beta^2)},$$
$$D_5=\frac{(9/16)K_{NL}}{I_0+I_2(\alpha^2+\beta^2)}. \quad (30)$$

According to the variational principle, solving Eq. (29) is equivalent to searching for $Q(t)$ that makes the following functional reach an extreme:

$$J(Q)=\int_0^{T/4}\left(-\frac{1}{2}\dot{W}^2+g_1\frac{W^2}{2}+g_2\frac{W^4}{4}\right)\mathrm{d}t, \quad (31)$$

where $g_1=D_1+D_2+D_3$, $g_2=D_4+D_5$, and T is the vibration period of the Kirchhoff microplate. The approximate sinusoidal solution can be written as [37]:

$$W(t)=\xi\cos(\omega t) \quad (32)$$

in which ξ and ω are the amplitude and frequency of the microplate, respectively. Substituting Eq. (32) into Eq. (31) and using the transformation $\theta=\omega t$, one obtains

$$J(\xi,\omega)=\frac{1}{\omega}\int_0^{\pi/2}\left(-\frac{1}{2}\xi^2\omega^2\sin^2\theta+\frac{g_1}{2}\xi^2\cos^2\theta+\frac{g_2}{4}\xi^4\cos^4\theta\right)\mathrm{d}\theta. \quad (33)$$

According to the Ritz method, the stationary conditions $\partial J/\partial\xi=0$ and $\partial J/\partial\omega=0$ should be satisfied to obtain ω. However, this approach is unable to give an accurate result for the present problem. To obtain the nonlinear vibration frequency, He [37] modified these conditions into a simpler form:

$$\frac{\partial J}{\partial\xi}=0. \quad (34)$$

According to this condition, the nonlinear vibration frequency of the Kirchhoff microplate is obtained as:

$$\omega_{KNL}=\sqrt{g_1+\frac{3}{4}g_2\xi^2}. \quad (35)$$

The linear natural frequency of the Kirchhoff microplate can be directly obtained from Eq. (29) as:

$$\omega_{KL}=\sqrt{g_1}. \quad (36)$$

Eq. (35) reveals that due to the intrinsic stiffening effect, the nonlinear vibration frequency of the FG microplate increases with the increase of the amplitude.

Obviously, for a free standing Kirchhoff microplate (i.e., $K_L=K_P=K_{NL}=0$), the linear natural frequency is

$$\omega_{KL}=(\alpha^2+\beta^2)\sqrt{\frac{D+A_n}{I_0+I_2(\alpha^2+\beta^2)}}, \quad (37)$$

which is identical to the result given in Ref. [32].

2.4. Analytical solutions for the deflection and frequency of the Mindlin microplate

The nonlinear bending and vibration problems of a simply supported FG microplate are investigated based on the MPT in this subsection. For the static bending problem of the FG microplate, the inertial terms in Eqs. (23) vanish. From Eqs. (22) and (23), one obtains:

$$\eta_{mn}=\frac{W_{1mn}}{W_{mn}}=\frac{A_{44}-(A_n/4)(\alpha^2+\beta^2)}{A_{44}+(D+A_n/4)(\alpha^2+\beta^2)}. \quad (38)$$

Substituting Eq. (38) into Eq. (23a), the nonlinear bending deflection of the Mindlin microplate subjected to a sinusoidal load of intensity q_0 can be obtained by solving the following algebraic equation:

$$\left\{\frac{A}{16}\left[4\nu\alpha^2\beta^2+(3-\nu^2)(\alpha^4+\beta^4)\right]+\frac{9}{16}K_{NL}\right\}W_{MNL}^3 + \left\{\left[\left(D+\frac{A_n}{2}\right)\eta_{11}+\frac{A_n}{2}\right](\alpha^2+\beta^2)^2+K_L+K_P(\alpha^2+\beta^2)\right\}W_{MNL}=q_0. \quad (39)$$

The real root of Eq. (39) is given as follows:

$$W_{MNL}=-a_2\left(\frac{27}{2}\bar{q}_0+\frac{3}{2}\sqrt{12a_2^3+81\bar{q}_0^2}\right)^{-1/3} + \left(\frac{1}{2}\bar{q}_0+\frac{1}{18}\sqrt{12a_2^3+81\bar{q}_0^2}\right)^{1/3}, \quad (40)$$

where

$$a_2=\frac{\left[(D+\frac{A_n}{2})\eta_{11}+\frac{A_n}{2}\right](\alpha^2+\beta^2)^2+K_L+K_P(\alpha^2+\beta^2)}{\frac{A}{16}\left[4\nu\alpha^2\beta^2+(3-\nu^2)(\alpha^4+\beta^4)\right]+\frac{9}{16}K_{NL}}. \quad (41)$$

If the shear stiffness A_{44} is set to be infinity, i.e., no shear deformation is allowed, the Mindlin microplate is degenerated to the Kirchhoff microplate. In this case, $\eta_{11} = 1$, and Eq. (40) gives the same result with Eq. (26).

The linear deflection of the Mindlin microplate can be expressed as:

$$W_{ML} = \frac{q_0}{[(D + A_n/2)\eta_{11} + A_n/2](\alpha^2 + \beta^2)^2 + K_L + K_P(\alpha^2 + \beta^2)}. \tag{42}$$

For the free vibration problem, Q_{mn} in Eqs. (23) vanishes. Solving the ODEs (23) is equivalent to searching for $W_1(t)$ and $W_2(t)$ that make the following functional reach an extreme:

$$\begin{aligned} J(W_1, W_2) = \int_0^{T/4} \Big[& k_{12}W_1W_2 + \frac{1}{2}k_{11}W_1^2 + \frac{1}{2}k_{22}W_2^2 \\ & + k_{13}\left(\frac{1}{4}W_1^4 + W_1^3W_2 + \frac{3}{2}W_1^2W_2^2 + W_1W_2^3 + \frac{1}{4}W_2^4\right) \\ & - m_{12}\dot{W}_1\dot{W}_2 - \frac{1}{2}m_{11}\dot{W}_1^2 - \frac{1}{2}m_{22}\dot{W}_2^2\Big]\mathrm{d}t. \end{aligned} \tag{43}$$

The approximate sinusoidal solutions of $W_1(t)$ and $W_2(t)$ are assumed as:

$$W_1(t) = \xi_1 \cos(\omega t), \quad W_2(t) = \xi_2 \cos(\omega t). \tag{44}$$

By substituting Eq. (44) into Eq. (43), one obtains

$$\begin{aligned} J(\xi_1, \xi_2, \omega) = \frac{\pi}{4\omega}\Big[& k_{12}\xi_1\xi_2 + \frac{1}{2}k_{11}\xi_1^2 + \frac{1}{2}k_{22}\xi_2^2 \\ & + \frac{3}{4}k_{13}\left(\frac{1}{4}\xi_1^4 + \xi_1^3\xi_2 + \frac{3}{2}\xi_1^2\xi_2^2 + \xi_1\xi_2^3 + \frac{1}{4}\xi_2^4\right) \\ & - \omega^2\left(m_{12}\xi_1\xi_2 + \frac{1}{2}m_{11}\xi_1^2 + \frac{1}{2}m_{22}\xi_2^2\right)\Big]. \end{aligned} \tag{45}$$

The stationary conditions $\partial J/\partial \xi_1 = 0$ and $\partial J/\partial \xi_2 = 0$ result in

$$\begin{cases} k_{11}\xi_1 + k_{12}\xi_2 + \frac{3}{4}k_{13}(\xi_1 + \xi_2)^3 - \omega^2(m_{11}\xi_1 + m_{12}\xi_2) = 0, \\ k_{12}\xi_1 + k_{22}\xi_2 + \frac{3}{4}k_{13}(\xi_1 + \xi_2)^3 - \omega^2(m_{12}\xi_1 + m_{22}\xi_2) = 0. \end{cases} \tag{46}$$

Define ξ and λ as $\xi = \xi_1 + \xi_2$ and $\lambda = \xi_1 - \xi_2$. Substituting $\xi_1 = (\xi + \lambda)/2$ and $\xi_2 = (\xi - \lambda)/2$ into Eq. (46) and eliminating the variable λ, the following equation is obtained:

$$c_1\omega^4 - (c_2 + c_3)\omega^2 + (c_4 + c_5) = 0 \tag{47}$$

in which

$$\begin{aligned} & c_1 = m_{11}m_{22} - m_{12}^2, \quad c_2 = k_{11}m_{22} + k_{22}m_{11} - 2k_{12}m_{12}, \\ & c_3 = \frac{3}{4}\xi^2k_{13}(m_{11} + m_{22} - 2m_{12}), \quad c_4 = k_{11}k_{22} - k_{12}^2, \\ & c_5 = \frac{3}{4}\xi^2k_{13}(k_{11} + k_{22} - 2k_{12}). \end{aligned} \tag{48}$$

The nonlinear vibration frequency of the Mindlin microplate is

$$\omega_{MNL} = \sqrt{\frac{1}{2c_1}\left\{(c_2 + c_3) - \left[(c_2 + c_3)^2 - 4c_1(c_4 + c_5)\right]^{1/2}\right\}}. \tag{49}$$

If the shear stiffness A_{44} is set to be infinity, the Mindlin microplate is degenerated to the Kirchhoff microplate. In this case, $k_{22} = \infty$, and Eq. (49) degenerates to

$$\omega_{KNL} = \sqrt{\frac{k_{11}}{m_{11}} + \frac{3}{4}\frac{k_{13}}{m_{11}}\xi^2}, \tag{50}$$

which gives the same result with Eq. (35).

The linear natural frequency of the Mindlin microplate is

$$\omega_{ML} = \sqrt{\frac{1}{2c_1}\left[c_2 - (c_2^2 - 4c_1c_4)^{1/2}\right]}. \tag{51}$$

3. Results and discussion

3.1. Validation studies

Since results for nonlinear bending and vibration of FG microplates are not available in the open literature, only the linear bending and free vibration problems of a free standing FG microplate and the nonlinear free vibration problem of a free standing macroscopic isotropic plate (i.e. $l = 0$, $p = 0$) are studied herein to validate the obtained closed-form solutions.

Example 1. Consider a simply supported square microplate with the following material properties [32]:

$$\begin{aligned} & E_1 = 14.4\ \text{GPa}, \quad E_2 = 1.44\ \text{GPa}, \quad \rho_1 = 12.2 \times 10^3\ \text{kg/m}^3, \\ & \rho_2 = 1.22 \times 10^3\ \text{kg/m}^3, \quad \nu = 0.38, \quad h = 17.6 \times 10^{-6}\ \text{m}, \\ & a/h = 10, \quad p = 1, \quad k_s = 5/6, \quad q_0 = 1.0\ \text{N/m}^2. \end{aligned}$$

The dimensionless deflection $\bar{w}$ and frequency $\bar{\omega}$ of the microplate are defined as:

$$\bar{w} = \frac{100E_2h^3}{q_0a^4}w\left(\frac{a}{2}, \frac{b}{2}\right), \quad \bar{\omega} = \omega\frac{a^2}{h}\sqrt{\frac{\rho_2}{E_2}}.$$

Tables 1 and 2 respectively list the results for linear bending and vibration of the FG microplate with various values of the material length scale parameter to thickness ratio l/h. The results obtained from the Kirchhoff and Mindlin plate theories are marked as "KPT" and "MPT", respectively. It can be seen from these tables that for linear bending and vibration problems, the present work gives the same results with those reported by Thai and Choi [32].

Example 2. Consider a simply supported macroscopic isotropic square plate with the following material properties [38]:

$$E = 322.2\ \text{GPa}, \quad \rho = 2370\ \text{kg/m}^3, \quad \nu = 0.3, \ a/h = 10.$$

Table 3 lists the ratios of the nonlinear vibration frequency of the plate to its linear counterpart for various values of the vibration amplitude. Both the nonlinear vibration frequency and the linear natural frequency are obtained by using the KPT. The same problem was also studied by Chen et al. who employed the Galerkin method and a Runge–Kutta method. Their results are also provided in the table for comparison. It is shown that the present work predicts comparable results with Chen et al. [38].

3.2. Parameter studies

In this subsection, the nonlinear bending/vibration behavior of a FG microplate is compared with its linear counterpart to clarify the effect of geometric nonlinearity. Furthermore, the influences of the material length scale parameter to thickness ratio, the length to thickness ratio, the power law index, and the elastic foundation

Table 1
Dimensionless deflection $\bar{w}$ of a simply supported square FG microplate.

l/h	KPT		MPT	
	Thai's results [32]	Present results	Thai's results [32]	Present results
0	0.6167	0.6167	0.6472	0.6472
0.2	0.5176	0.5176	0.5433	0.5433
0.4	0.3492	0.3492	0.3678	0.3678
0.6	0.2264	0.2264	0.2406	0.2406
0.8	0.1517	0.1517	0.1635	0.1635
1.0	0.1065	0.1065	0.1169	0.1169

Table 2
Dimensionless frequency $\bar{\omega}$ of a simply supported square FG microplate.

l/h	KPT		MPT	
	Thai's results [32]	Present results	Thai's results [32]	Present results
First mode				
0	5.3953	5.3953	5.2697	5.2697
0.2	5.8894	5.8894	5.7518	5.7518
0.4	7.1702	7.1702	6.9920	6.9920
0.6	8.9045	8.9045	8.6477	8.6477
0.8	10.8775	10.8775	10.4942	10.4942
1.0	12.9808	12.9808	12.1428	12.4128
Second mode				
0	13.3625	13.3625	12.6460	12.6460
0.2	14.5861	14.5861	13.8057	13.8057
0.4	17.7583	17.7583	16.7603	16.7603
0.6	22.0536	22.0536	20.6375	20.6375
0.8	26.9400	26.9400	24.8597	24.8597
1.0	32.1492	32.1492	29.1174	29.1174

Table 3
Ratio of the nonlinear vibration frequency to the linear natural frequency of an isotropic plate.

	ξ/h				
	0.2	0.4	0.6	0.8	1.0
Chen's results [38]	1.017	1.084	1.188	1.310	1.362
Present results	1.020	1.076	1.164	1.277	1.410

on the nonlinear bending and vibration responses of the FG microplate are studied comprehensively.

Consider a free standing simply supported square FG microplate with the following material properties:

$$E_1 = 14.4\ \text{GPa}, \quad E_2 = 1.44\ \text{GPa}, \quad \rho_1 = 12.2 \times 10^3\ \text{kg/m}^3,$$
$$\rho_2 = 1.22 \times 10^3\ \text{kg/m}^3, \quad \nu = 0.38, \quad h = 17.6 \times 10^{-6}\ \text{m}.$$

The dimensionless load parameter and frequency are defined as follows:

$$\bar{P} = \frac{q_0 a^4}{E_1 h^4}, \quad \bar{\omega} = \omega \frac{a^2}{h}\sqrt{\frac{\rho_2}{E_2}}.$$

To study the effect of geometric nonlinearity on the responses of the FG microplate, its nonlinear bending/vibration behavior and linear counterpart are compared. Fig. 2 depicts the linear and nonlinear bending deflection-load curves of the microplate under sinusoidal loads, and Fig. 3 shows the linear and nonlinear vibration frequency–amplitude curves of the microplate. It is observed that the nonlinear bending deflection is smaller than its linear counterpart under the action of the same load, while the nonlinear vibration frequency is higher than its linear counterpart for the same amplitude. These phenomena are attributed to the intrinsic stiffening effect of the microplate brought by geometric nonlinearity, as explained in Section 2.3. Moreover, one can find that the nonlinear frequency gets larger with the increase of the amplitude. This is also due to the intrinsic stiffening effect. Figs. 2 and 3 show the differences between the two groups of results predicted respectively by the Kirchhoff and Mindlin plate theories as well. As expected, the KPT underestimates the bending deflection and overestimates the vibration frequency due to neglecting the transverse shear deformation.

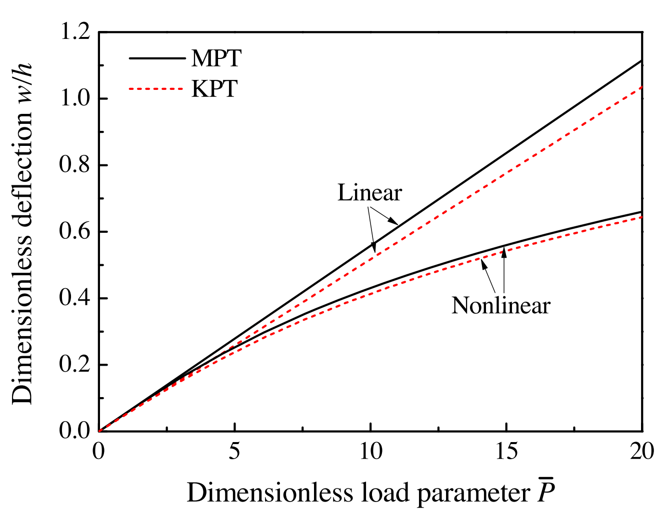

Fig. 2. Linear and nonlinear bending deflection–load curves of the FG microplate ($a/h = 8$, $l/h = 0.2$, $p = 1$).

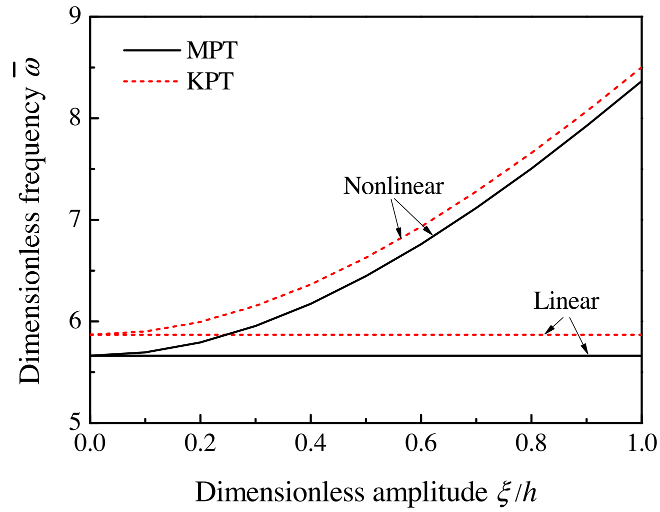

Fig. 3. Linear and nonlinear vibration frequency–amplitude curves of the FG microplate ($a/h = 8$, $l/h = 0.2$, $p = 1$).

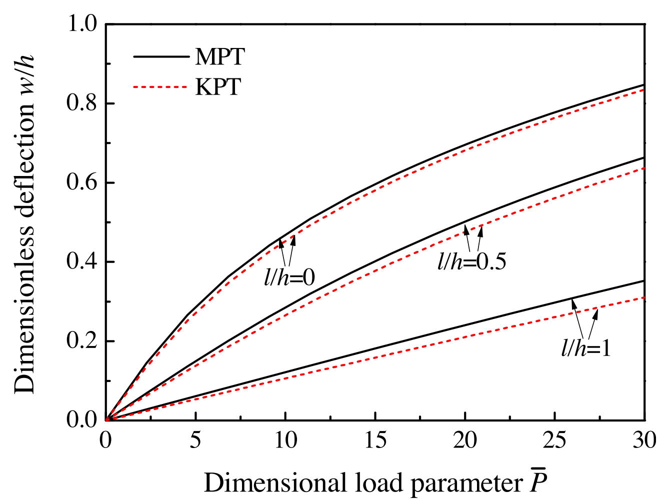

Fig. 4. Effect of the material length scale parameter to thickness ratio on the nonlinear bending deflection of the FG microplate ($a/h = 8$, $p = 1$).

Figs. 4 and 5 illustrate the effect of the material length scale parameter to thickness ratio l/h on the nonlinear bending and vibration responses of the microplate. It shows clearly that the deflection decreases and the frequency increases with the increase of l/h. This can be explained as follows. According to the MCST,

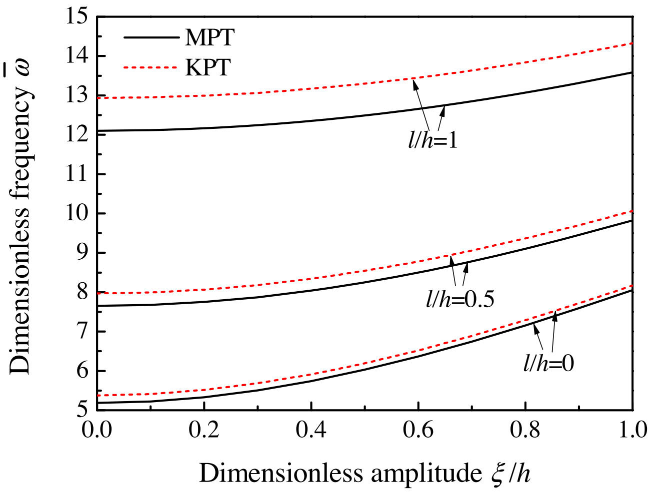

Fig. 5. Effect of the material length scale parameter to thickness ratio on the nonlinear vibration frequency of the FG microplate ($a/h = 8,\ p = 1$).

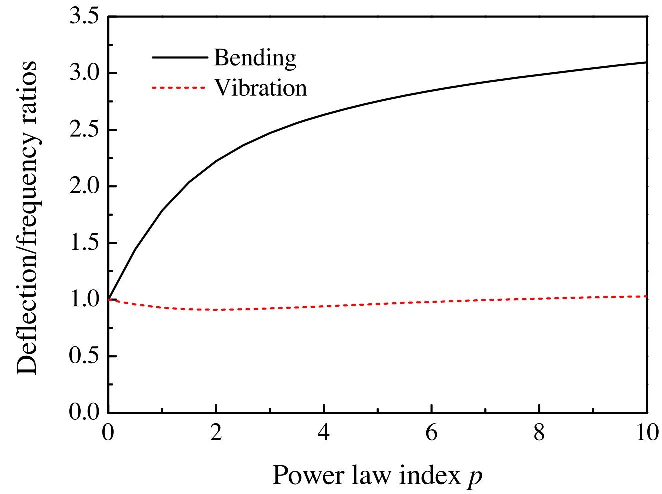

Fig. 8. Effect of the power law index on the ratio of the deflection (frequency) of the FG microplate to its isotropic counterpart ($a/h = 8,\ l/h = 0.2,\ q_0 = 40$ MPa, $\xi = 0.5h$).

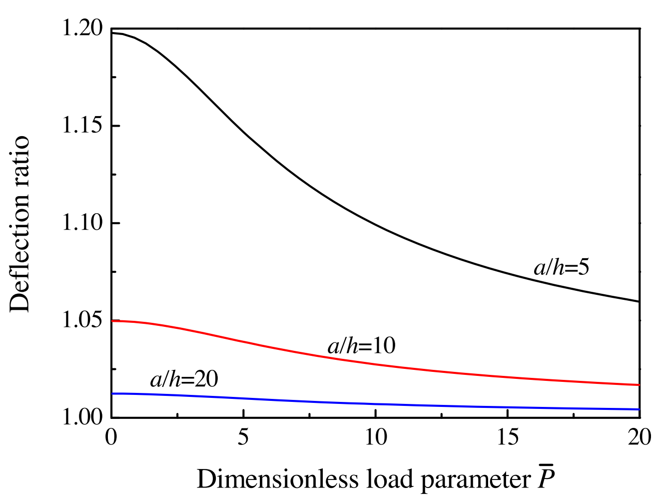

Fig. 6. Effect of the length to thickness ratio on the ratio of the deflection predicted by the Mindlin plate theory to that predicted by the Kirchhoff plate theory ($l/h = 0.2,\ p = 1$).

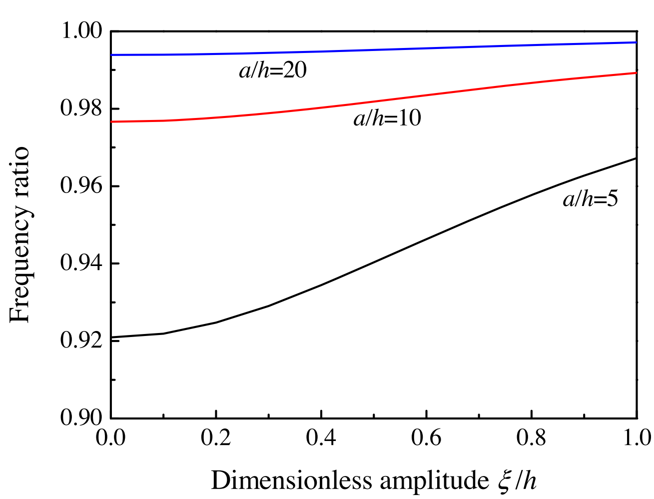

Fig. 7. Effect of the length to thickness ratio on the ratio of the frequency predicted by the Mindlin plate theory to that predicted by the Kirchhoff plate theory ($l/h = 0.2,\ p = 1$).

couple stress is needed to generate the gradient of rotation. The stiffness owing to the couple stress effect is added to the classical stiffness, thus the total stiffness of the microplate is larger than its classical counterpart (i.e., $l = 0$). In addition, with the increase of l/h, the couple stress effect becomes more significant, thus the stiffness of the microplate increases, which leads to the decrease of the deflection and the increase of the frequency. It is also

Table 4
Dimensionless deflection w/h of a free standing square FG microplate.

a/h	p	l/h	$\bar{P}=5$	$\bar{P}=10$	$\bar{P}=15$	$\bar{P}=20$	$\bar{P}=25$	$\bar{P}=30$
5	1	0	0.3082	0.4911	0.6170	0.7146	0.7953	0.8647
		0.2	0.2739	0.4549	0.5827	0.6824	0.7649	0.8357
		0.4	0.2014	0.3645	0.4916	0.5941	0.6801	0.7543
		0.6	0.1387	0.2666	0.3791	0.4769	0.5624	0.6380
		0.8	0.0982	0.1934	0.2834	0.3671	0.4444	0.5156
		1.0	0.0733	0.1456	0.2161	0.2842	0.3494	0.4116
	5	0	0.4994	0.7310	0.8867	1.0073	0.1073	0.1937
		0.2	0.4653	0.7006	0.8592	0.9820	1.0837	1.1714
		0.4	0.3794	0.6166	0.7817	0.9100	1.0160	1.1072
		0.6	0.2834	0.5033	0.6700	0.8030	0.9139	1.0094
		0.8	0.2087	0.3938	0.5497	0.6811	0.7936	0.8920
		1.0	0.1585	0.3083	0.4443	0.5660	0.6744	0.7716
	10	0	0.5629	0.8196	0.9919	1.1255	1.2364	1.3322
		0.2	0.5329	0.7930	0.9681	1.1037	1.2160	1.3129
		0.4	0.4541	0.7187	0.9002	1.0408	1.1570	1.2570
		0.6	0.3575	0.6132	0.7992	0.9454	1.0667	1.1710
		0.8	0.2736	0.5018	0.6836	0.8318	0.9566	1.0647
		1.0	0.2125	0.4058	0.5731	0.7166	0.8411	0.9506
10	1	0	0.2824	0.4641	0.5916	0.6908	0.7728	0.8433
		0.2	0.2482	0.4252	0.5538	0.6549	0.7387	0.8107
		0.4	0.1780	0.3303	0.4542	0.5564	0.6429	0.7180
		0.6	0.1191	0.2321	0.3352	0.4278	0.5107	0.5852
		0.8	0.0815	0.1615	0.2389	0.3128	0.3827	0.4486
		1.0	0.0584	0.1164	0.1737	0.2298	0.2847	0.3380
	5	0	0.4675	0.7025	0.8610	0.9837	1.0853	1.1728
		0.2	0.4308	0.6683	0.8298	0.9548	1.0582	1.1472
		0.4	0.3406	0.5739	0.7408	0.8713	0.9793	1.0722
		0.6	0.2444	0.4488	0.6121	0.7453	0.8576	0.9549
		0.8	0.1728	0.3335	0.4766	0.6021	0.7126	0.8107
		1.0	0.1257	0.2478	0.3636	0.4715	0.5713	0.6634
	10	0	0.5203	0.7817	0.9578	1.0942	1.2072	1.3045
		0.2	0.4874	0.7511	0.9301	1.0685	1.1831	1.2818
		0.4	0.4030	0.6654	0.8500	0.9938	1.1127	1.2149
		0.6	0.3045	0.5453	0.7302	0.8783	1.0021	1.1088
		0.8	0.2233	0.4237	0.5945	0.7396	0.8646	0.9740
		1.0	0.1661	0.3245	0.4702	0.6019	0.7206	0.8277

Table 5
Dimensionless frequency $\bar{\omega}$ of a free standing square FG microplate.

a/h	p	l/h	$\xi/h = 0$	$\xi/h = 0.2$	$\xi/h = 0.4$	$\xi/h = 0.6$	$\xi/h = 0.8$	$\xi/h = 1.0$
5	1	0	4.8744	5.0249	5.4515	6.0964	6.8986	7.8097
		0.2	5.3239	5.4622	5.8574	6.4626	7.2251	8.1004
		0.4	6.4600	6.5748	6.9076	7.4293	8.1034	8.8951
		0.6	7.9298	8.0240	8.3003	8.7412	9.3236	10.0226
		0.8	9.4998	9.5790	9.8128	10.1906	10.6971	11.3150
		1.0	11.0451	11.1137	11.3171	11.6480	12.0962	12.6490
	5	0	5.1186	5.2617	5.6693	6.2902	7.0682	7.9572
		0.2	5.5399	5.6726	6.0530	6.6387	7.3809	8.2373
		0.4	6.6194	6.7312	7.0558	7.5660	8.2271	9.0058
		0.6	8.0368	8.1295	8.4017	8.8366	9.4116	10.1029
		0.8	9.5671	9.6456	9.8774	10.2521	10.7547	11.3682
		1.0	11.0847	11.1530	11.3553	11.6847	12.1308	12.6813
	10	0	5.5818	5.7126	6.0880	6.6668	7.4012	8.2497
		0.2	5.9551	6.0780	6.4325	6.9835	7.6886	8.5095
		0.4	6.9333	7.0395	7.3490	7.8375	8.4742	9.2282
		0.6	8.2517	8.3417	8.6059	9.0291	9.5900	10.2661
		0.8	9.7045	9.7816	10.0094	10.3779	10.8728	11.4776
		1.0	11.1666	11.2342	11.4345	11.7607	12.2027	12.7485
10	1	0	5.2697	5.4125	5.8201	6.4422	7.2238	8.1189
		0.2	5.7518	5.8830	6.2600	6.8423	7.5829	8.4400
		0.4	6.9920	7.1003	7.4158	7.9137	8.5622	9.3301
		0.6	8.6477	8.7356	8.9940	9.4089	9.9609	10.6285
		0.8	10.4942	10.5667	10.7815	11.1302	11.6008	12.1792
		1.0	12.4128	12.4743	12.6568	12.9554	13.3622	13.8677
	5	0	5.5800	5.7150	6.1018	6.6971	7.4511	8.3206
		0.2	6.0343	6.1593	6.5199	7.0802	7.7973	8.6321
		0.4	7.2185	7.3234	7.6292	8.1134	8.7464	9.4984
		0.6	8.8219	8.9080	9.1612	9.5684	10.1110	10.7685
		0.8	10.6274	10.6989	10.9109	11.2552	11.7203	12.2924
		1.0	12.5148	12.5757	12.7566	13.0526	13.4561	13.9576
	10	0	6.1903	6.3118	6.6632	7.2108	7.9141	8.7355
		0.2	6.5967	6.7109	7.0424	7.5627	8.2361	9.0283
		0.4	7.6797	7.7780	8.0659	8.5241	9.1271	9.8482
		0.6	9.1829	9.2653	9.5085	9.9004	10.4244	11.0617
		0.8	10.9066	10.9761	11.1823	11.5177	11.9715	12.5308
		1.0	12.7303	12.7900	12.9675	13.2581	13.6546	14.1481

observed from Figs. 4 and 5 that the effect of the transverse shear deformation is more significant when the couple stress effect is considered. Similar phenomenon was also reported by Thai and Choi for the case of linear bending and vibration of FG microplates [32].

Figs. 6 and 7 depict the effect of the length to thickness ratio a/h on the nonlinear bending and vibration responses of the FG microplate. In Fig. 6 (Fig. 7), the deflection (frequency) ratio is defined as the ratio of the deflection (frequency) predicted by the MPT to that predicted by the KPT. It shows that both the deflection and frequency ratios approach to 1 with the increase of a/h. Moreover, the calculated results demonstrate that for FG microplates with length to thickness ratio larger than 20, the error caused by neglecting the transverse shear deformation is within 1.5%, thus, in this case the KPT may give an acceptable result for engineering applications.

Fig. 8 illustrates the influence of the power law index p on the nonlinear bending and vibration responses of the FG microplate. The results shown in this figure are calculated based on the MPT, and the deflection (frequency) ratio is defined as the ratio of the deflection (frequency) of the FG microplate to its isotropic counterpart (i.e., $p = 0$). Fig. 8 reveals that the bending deflection increases with the increase of the power law index. This is because that with the increase of p, the volume fraction of the stiffer material (Material 1) becomes smaller, hence the stiffness of the FG microplate decreases and the deflection increases. Fig. 8 also shows that the vibration frequency varies slightly with p. Although the stiffness of the FG microplate decreases with the increase of p, the density also decreases, as a result the stiffness to mass ratio varies slightly with the power law index, which leads to a small change of the vibration frequency.

The nonlinear bending deflection and vibration frequency of a free standing FG microplate with different material length scale parameter to thickness ratios, length to thickness ratios, and power law indexes, which are calculated by the MPT, are given in Tables 4 and 5 respectively. Similar conclusions for the effects of these parameters on the bending and vibration behavior of the FG microplate can also be drawn from these tables.

Table 6
Dimensionless deflection w/h of a square FG microplate lying on an elastic foundation.

$\bar{P}$	$\bar{K}_L = \bar{K}_P = 0,\ \bar{K}_{NL} = 0$	$\bar{K}_L = \bar{K}_P = 0,\ \bar{K}_{NL} = 100$	$\bar{K}_L = \bar{K}_P = 0,\ \bar{K}_{NL} = 200$	$\bar{K}_L = \bar{K}_P = 10,\ \bar{K}_{NL} = 200$	$\bar{K}_L = \bar{K}_P = 20,\ \bar{K}_{NL} = 200$
5	0.2532	0.2333	0.2195	0.1697	0.1350
10	0.4312	0.3723	0.3390	0.2870	0.2431
15	0.5598	0.4680	0.4202	0.3711	0.3266
20	0.6606	0.5423	0.4830	0.4370	0.3938
25	0.7441	0.6036	0.5350	0.4915	0.4500
30	0.8159	0.6564	0.5797	0.5384	0.4984

($a/h = 8,\ l/h = 0.2,\ p = 1$).

Table 7
Dimensionless frequency $\bar{\omega}$ of a square FG microplate lying on an elastic foundation.

ξ/h	$\overline{K}_L = \overline{K}_P = 0, \overline{K}_{NL} = 0$	$\overline{K}_L = \overline{K}_P = 0,\ \overline{K}_{NL} = 100$	$\overline{K}_L = \overline{K}_P = 0,\ \overline{K}_{NL} = 200$	$\overline{K}_L = \overline{K}_P = 10,\ \overline{K}_{NL} = 200$	$\overline{K}_L = \overline{K}_P = 20,\ \overline{K}_{NL} = 200$
0	5.6615	5.6615	5.6615	6.8907	7.9317
0.2	5.7940	5.9590	6.1196	7.2718	8.2648
0.4	6.1745	6.7736	7.3238	8.3107	9.1921
0.6	6.7611	7.9477	8.9788	9.8004	10.5582
0.8	7.5058	9.3469	10.8807	11.5679	12.2165
1.0	8.3664	10.8846	12.9208	13.5046	14.0641

$(a/h = 8,\ l/h = 0.2,\ p = 1)$.

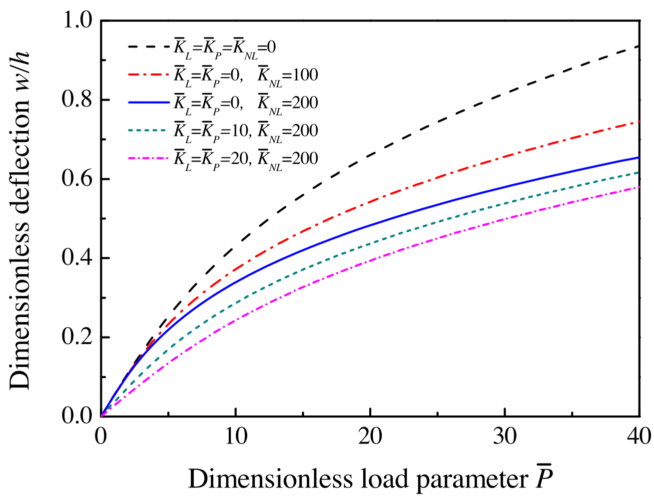

Fig. 9. Effect of the elastic foundation on the nonlinear bending deflection $(a/h = 8,\ l/h = 0.2,\ p = 1)$.

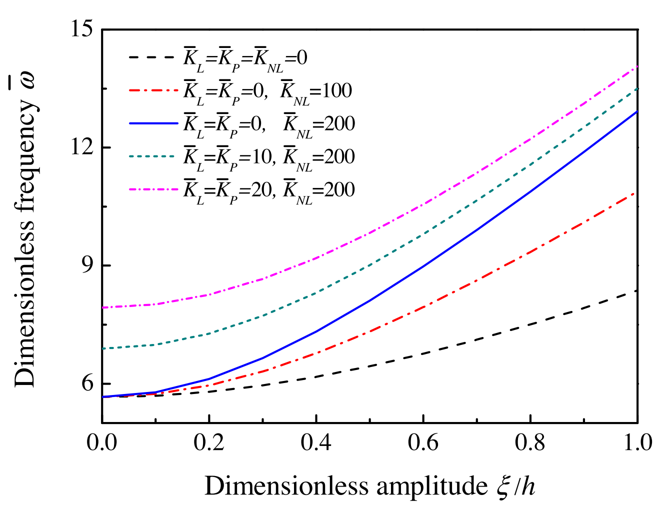

Fig. 10. Effect of the elastic foundation on the nonlinear vibration frequency $(a/h = 8,\ l/h = 0.2,\ p = 1)$.

Figs. 9 and 10 show the effect of the elastic foundation on the nonlinear bending deflection and vibration frequency of the FG microplate. The dimensionless stiffness coefficients are defined as:

$$\overline{K}_L = \frac{K_L a^4}{D}, \quad \overline{K}_P = \frac{K_P a^2}{D}, \quad \overline{K}_{NL} = \frac{K_{NL} a^4}{A}.$$

It is evident that the increase of these stiffness coefficients leads to the decrease of the bending deflection and the increase of the vibration frequency. This is attributed to the increase of the stiffness contributed by the elastic foundation. Moreover, comparison among the frequency–amplitude curves in Fig. 10 demonstrates that, for a FG microplate lying on elastic foundations with the same transverse stiffness coefficient K_L, shear stiffness coefficient K_P, but different nonlinear stiffness coefficient K_{NL}, as the amplitude approaches to zero, the nonlinear vibration frequencies tend towards a fixed value. This phenomenon can be interpreted as follows. When the amplitude is close to zero, the intrinsic stiffening effect of the FG microplate and the contribution of the nonlinear stiffness of the foundation are negligible, as a result, the nonlinear vibration frequency coincides with the linear natural frequency, which is independent of the nonlinear stiffness of the foundation.

The nonlinear bending deflection and vibration frequency of the FG microplate lying on elastic foundations with different stiffness coefficients are also given in Tables 6 and 7. These data can be used as a reference for further studies.

4. Conclusions

This paper investigates the nonlinear bending and free vibration behavior of a functionally graded (FG) microplate lying on an elastic foundation by using the modified couple stress theory and the Kirchhoff/Mindlin plate theory. The von Karman's nonlinear strain–displacement relationship and the nonlinear stiffness of the elastic foundation are the sources of nonlinearity of the considered problems. The equations of motion and boundary conditions of the FG microplate are derived from the Hamilton's principle. Due to introducing the physical neutral surface, there is no stretching-bending coupling in the constitutive equations, and consequently the equations of motion of the FG microplate take similar forms with those of a homogeneous isotropic microplate. By using the Galerkin approach, the equations of motion are reduced to nonlinear algebraic equations and ordinary differential equations for the bending and free vibration problems respectively. Analytical solutions for the nonlinear bending deflection of the microplate are derived by solving the algebraic equations, and analytical formulas for the nonlinear vibration frequency of the microplate are also obtained by applying He's variational method to the ordinary differential equations. Comparison between the results predicted respectively by the Kirchhoff and Mindlin plate theories reveals that when the shear stiffness of the FG microplate is set to be infinity, the solutions obtained by using the Mindlin plate theory coincide with those obtained by using the Kirchhoff plate theory.

The correctness of the obtained solutions is validated by comparing them with available results in the open literature. Furthermore, the effects of various parameters on the nonlinear bending and vibration responses of the microplate are also investigated. It is found that due to the intrinsic stiffening effect of the microplate brought by geometric nonlinearity, the nonlinear bending deflection is smaller than its linear counterpart under the action of the same load, while the nonlinear vibration frequency is higher than its linear counterpart for the same amplitude. It is also revealed that attributed to the contribution of the couple stress effect, the stiffness of the microplate is larger than its classical counterpart (i.e., $l = 0$). Moreover, the couple stress effect is more significant for microplate with a larger material length scale parameter to thickness ratio.

It is expected that the derived analytical formulas for the nonlinear bending deflection and vibration frequency can be used to characterize the nonlinear mechanical behavior and the size effects of FG microplates prevalently applied in micro/nano engineering fields. Moreover, the solution techniques presented in this paper can also be utilized to derive closed-form solutions for nonlinear bending deflection and vibration frequency of higher-order shear deformable FG microplates.

Acknowledgment

The present work is supported by the National Science Foundation of China under Grant Nos. 11172080 and 11202059 and sponsored by K.C. Wong Magna Fund in Ningbo University.

References

[1] Shen HS. A comparison of buckling and postbuckling behavior of FGM plates with piezoelectric fiber reinforced composite actuators. Compos Struct 2009;91:375–84.
[2] Latifi M, Farhatnia F, Kadkhodaei M. Buckling analysis of rectangular functionally graded plates under various edge conditions using Fourier series expansion. Eur J Mech A/Solids 2013;41:16–27.
[3] Ke LL, Yang J, Kitipornchai S, Wang YS. Axisymmetric postbuckling analysis of size-dependent functionally graded annular microplates using the physical neutral plane. Int J Eng Sci 2014;81:66–81.
[4] Eringen AC. Nonlocal polar elastic continua. Int J Eng Sci 1972;10:1–16.
[5] Lam DCC, Yang F, Chong ACM, Wang J, Tong P. Experiments and theory in strain gradient elasticity. J Mech Phys Solids 2003;51:1477–508.
[6] Aifantics EC. Strain gradient interpretation of size effects. Int J Fract 1999;95:1–4.
[7] Toupin RA. Elastic materials with couple-stresses. Arch Ration Mech Anal 1962;11(1):385–414.
[8] Mindlin RD, Tiersten HF. Effects of couple-stresses in linear elasticity. Arch Ration Mech Anal 1962;11(1):415–48.
[9] Mindlin RD. Influence of couple-stresses on stress concentrations. Exp Mech 1963;3:1–7.
[10] Yang F, Chong ACM, Lam DCC, Tong P. Couple stress based strain gradient theory for elasticity. Int J Solids Struct 2002;39(10):2731–43.
[11] Park SK, Gao XL. Bernoulli–Euler beam model based on a modified couple stress theory. J Micromech Microeng 2006;16:2355–9.
[12] Kong S, Shou S, Nie Z, Wang K. The size-dependent natural frequency of Bernoulli–Euler micro-beams. Int J Eng Sci 2008;46(5):427–37.
[13] Kahrobaiyan MH, Asghari M, Rahaeifard M, Ahmadian MT. Investigation of the size-dependent dynamic characteristics of atomic force microscope microcantilevers based on a modified couple theory. Int J Eng Sci 2010;48(12):1985–94.
[14] Ma HM, Gao XL, Reddy JN. A microstructure-dependent Timoshenko beam model based on a modified couple stress theory. J Mech Phys Solids 2008;56(12):3379–91.
[15] Fu Y, Zhang J. Modeling and analysis of microtubules based on a modified couple stress theory. Physica E: Low-dimensional Syst Nanostruct 2010;42(5):1741–5.
[16] Ke LL, Wang YS. Flow-induced vibration and instability of embedded double-walled carbon nanotubes based on a modified couple stress theory. Physica E: Low-dimensional Syst Nanostruct 2011;43(5):1031–9.
[17] Ma HM, Gao XL, Reddy JN. A nonclassical Reddy–Levinson beam model based on a modified couple stress theory. Int J Multiscale Comput Eng 2010;8(2):167–80.
[18] Tsiatas GC. A new Kirchhoff plate model based on a modified couple stress theory. Int J Solids Struct 2009;46:2757–64.
[19] Jomehzadeh E, Noori HR, Saidi AR. The size-dependent vibration analysis of micro-plates based on a modified couple stress theory. Phys E: Low-dimensional Syst Nanostruct 2011;43(4):877–83.
[20] Yin L, Xia W, Wang L, Qian Q. Vibration analysis of microscale plates based on modified couple stress theory. Acta Mech Solida Sin 2010;23:386–93.
[21] Ke LL, Wang YS, Yang J, Kitipornchai S. Free vibration of size-dependent Mindlin microplates based on the modified couple stress theory. J Sound Vib 2012;331:94–106.
[22] Thai HT, Kim SE. A size-dependent functionally graded Reddy plate model based on a modified couple stress theory. Compos Part B: Eng 2013;45:1636–45.
[23] Kim J, Reddy JN. Analytical solutions for bending, vibration, and buckling of FGM plates using a couple stress-based third-order theory. Compos Struct 2013;103:86–98.
[24] Xia W, Wang L, Yin L. Nonlinear non-classical microscale beams: static bending, postbuckling and free vibration. Int J Eng Sci 2010;48(12):2044–53.
[25] Simsek M. Nonlinear static and free vibration analysis of microbeams based on the nonlinear elastic foundation using modified couple stress theory and He's variational method. Compos Struct 2014;112:264–72.
[26] Asghari M, Kahrobaiyan MH, Ahmadian MT. A nonlinear Timoshenko beam formulation based on the modified couple stress theory. Int J Eng Sci 2010;48(12):1749–61.
[27] Reddy JN, Berry J. Nonlinear theories of axisymmetric bending of functionally graded circular plates with modified couple stress. Compos Struct 2012;94(12):3664–8.
[28] Wang YG, Lin WH, Liu N. Large amplitude free vibration of size-dependent circular microplates based on the modified couple stress theory. Int J Mech Sci 2013;71:51–7.
[29] Ke LL, Yang J, Kitipornchai S, Bradford MA, Wang YS. Axisymmetric nonlinear free vibration of size-dependent functionally graded annular microplates. Compos Part B: Eng 2013;53:207–17.
[30] Ansari R, Shojaei MF, Mohammadi V, Gholami R, Darabi MA. Nonlinear vibrations of functionally graded Mindlin microplates based on the modified couple stress theory. Compos Struct 2014;114:124–34.
[31] Reddy JN, Kim J. A nonlinear modified couple stress-based third-order theory of functionally graded plates. Compos Struct 2012;94:1128–43.
[32] Thai HT, Choi DH. Size-dependent functionally graded Kirchhoff and Mindlin plate models based on a modified couple stress theory. Compos Struct 2013;95:142–53.
[33] Abrate S. Functionally graded plates behave like homogeneous plates. Compos Part B: Eng 2008;39:151–8.
[34] Emam SA, Nayfeh AH. Postbuckling and free vibrations of composite beams. Compos Struct 2009;88:636–42.
[35] Emam SA. A static and dynamic analysis of the postbuckling of geometrically imperfect composite beam. Compos Struct 2009;90:247–53.
[36] Niyogi AK. Nonlinear bending of rectangular orthotropic plates. Int J Solids Struct 1973;9(9):1133–9.
[37] He JH. Variational approach for nonlinear oscillators. Chaos Solitons Fract 2007;34:1430–9.
[38] Chen CS, Chen TJ, Chien RD. Nonlinear vibration of initially stressed functionally graded plates. Thin-Walled Struct 2006;44:844–51.